Published in final edited form as:
Int J Ion Mobil Spectrom. 2003 June 1; 16(2): 85–94. doi:10.1007/s12127-013-0123-7.

The Influence of Drift Gas Composition on the Separation Mechanism in Traveling Wave Ion Mobility Spectrometry: Insight from Electrodynamic Simulations

Jody C. May and **John A. McLean**
Department of Chemistry, Vanderbilt Institute of Chemical Biology, Vanderbilt Institute for Integrative Biosystems Research and Education, Vanderbilt University, Nashville, TN 37235-1822, USA

Abstract

The influence of three different drift gases (helium, nitrogen, and argon) on the separation mechanism in traveling wave ion mobility spectrometry is explored through ion trajectory simulations which include considerations for ion diffusion based on kinetic theory and the electrodynamic traveling wave potential. The model developed for this work is an accurate depiction of a second-generation commercial traveling wave instrument. Three ion systems (cocaine, MDMA, and amphetamine) whose reduced mobility values have previously been measured in different drift gases are represented in the simulation model. The simulation results presented here provide a fundamental understanding of the separation mechanism in traveling wave, which is characterized by three regions of ion motion: (1) ions surfing on a single wave, (2) ions exhibiting intermittent roll-over onto subsequent waves, and (3) ions experiencing a steady state roll-over which repeats every few wave cycles. These regions of ion motion are accessed through changes in the gas pressure, wave amplitude, and wave velocity. Resolving power values extracted from simulated arrival times suggest that momentum transfer in helium gas is generally insufficient to access regions (2) and (3) where ion mobility separations occur. Ion mobility separations by traveling wave are predicted to be effectual for both nitrogen and argon, with slightly lower resolving power values observed for argon as a result of band-broadening due to collisional scattering. For the simulation conditions studied here, the resolving power in traveling wave plateaus between regions (2) and (3), with further increases in wave velocity contributing only minor improvements in separations.

Keywords

traveling wave ion mobility spectrometry; TWIMS resolving power; electrodynamic ion simulations; alternate drift gases; helium; nitrogen; argon

INTRODUCTION

Traveling wave ion mobility spectrometry (TWIMS) is a gas-phase separation technique which utilizes an electrodynamic potential waveform applied across a gas-filled region in order to obtain a mobility spectrum (Shvartsburg and Smith 2008; Giles et al. 2004; Pringle et al. 2007). TWIMS shares parallels with conventional drift tube ion mobility spectrometry (DTIMS) in that the resulting mobility separation in both techniques are recorded as a time-dispersed arrival time spectrum. The primary differences between TWIMS and conventional DTIMS are in the mode of operation: TWIMS utilizes a low voltage (10 to 40 V) traveling wave pulse to intermittently drive ions axially through a reduced pressure (1 to 3 Torr) drift region (Giles et al. 2004; Giles et al. 2011; Pringle et al. 2007), whereas DTIMS utilizes a uniform field potential gradient (up to several thousand volts) to provide a constant driving

force for axial ion motion. Unlike TWIMS, DTIMS is routinely operated as a stand-alone spectrometer under ambient pressure (*ca.* 760 Torr) conditions. The reduced pressures and voltages used in the TWIMS device are a result of the technology being developed as a component for IM-MS instrument integration, and as such there has not been strong motivation for adapting the technology to other modes of operation, such as elevated pressures and various drift gas compositions. Additionally, the TWIMS experimental parameters are optimized for nitrogen drift gas, which is readily available and provides adequate drag force on the ion to effectuate ion mobility separations in the device. Thus, questions remain regarding the effectiveness of the traveling wave-based separation mechanisms when various drift gas compositions are utilized.

It has been demonstrated that the selection of drift gas in conventional DTIMS can have a profound effect on the observed ion mobility separations, specifically by altering the selectivity of the separation. For example, Hill and coworkers have demonstrated that isomers which cannot be resolved in nitrogen or ambient air can be separated in other drift gases such as argon and CO_2 (Asbury and Hill 2000). Changes in selectivity were attributed to both the mass and the polarizability of the drift gas. Ruotolo et al. have explored various drift gas compositions for improving the peak capacity and separation of peptides within a relatively wide mass range (500-3500 Da) (Ruotolo et al. 2004). They found that nitrogen and methane yielded the greatest peak capacity, whereas argon exhibited the poorest peak capacity as a result of the decreased sensitivity due to collisional scatter losses within the drift tube.

In more dramatic examples, doping the drift gas with a small amount of neutral modifier agent can effectuate the separation of structural (Rusyniak et al. 2003) and chiral isomers (Dwivedi et al. 2006). This separation enhancement is a result of intrinsic differences in the ion-neutral interaction which in turn alters the mobilities, and by association, the collision cross-section of the ions differently. For analytes within a relatively narrow mass range, such as drug compounds, the differences in collision cross-sections are minor and the contribution of band-broadening due to normal ion-gas diffusion is high, making it challenging to separate such analytes by their gas-phase ion mobilities. Previous experiments by Matz et al. explored the utility of several drift gases (helium, nitrogen, argon, and carbon dioxide) on separating several classes of drug compounds in an ambient pressure DTIMS (Matz et al. 2002). Their experimental findings demonstrate that compounds with different chemical properties (i.e., different chemical classes) can be better separated in the more polar carbon monoxide than the other gases explored, while, helium drift gas offered a better enhancement in separation for compounds exhibiting similar chemical properties (*i.e.*, molecules within the same class). Recent studies by Creaser and coworkers explored the use of these same set of drift gases in a first-generation TWIMS for separating drug compounds representing a narrow mass range between 230 and 382 Da (Howdle et al. 2010). No separations were reported for helium, whereas slightly better resolution was observed in pure argon than in pure nitrogen or carbon dioxide for all pressure conditions evaluated. Binary gas mixtures were also explored, with the highest resolution between two drug compounds (Rosiglitazone and Lamotrigine, m/z 358 and 256, respectively) occurring for TWIMS separations conducted in *ca.* 80% argon mixed with nitrogen gas. Of note in this work was that the argon/nitrogen gas mixtures exhibited higher resolution of the test compounds than did pure argon, suggesting that, as with conventional DTIMS, a balance exists in TWIMS between enhanced selectivity and band-broadening for achieving optimal separations.

Here we present ion simulation results which critically explore both the nature and the extent of ion separation in an *in silico* TWIMS device for three different drift gases (helium, nitrogen and argon).

A Brief Overview of the Separation Mechanism in Traveling Wave IMS

The electrode geometry of a TWIMS drift cell is similar to that of a conventional DTIMS, as both utilize a stacked ring ion guide contained within a gas-filled region (Figure 1A) (Giles et al. 2004; Pringle et al. 2007; Giles et al. 2011; Giles et al. 2010). The primary differences between DTIMS and TWIMS is the manner in which the potentials are applied (electrostatic and electrodynamic, respectively). In TWIMS, a dynamically-pulsed potential is applied to the drift cell and rapidly switched from front to back, creating a traveling wave potential that propels ions through the device (Figure 1B). Once captured by the traveling waves, one of two general modes of ion motion occur within TWIMS. (1) Either the ion is sufficiently mobile to keep up with the switching velocity of the traveling wave, and thus "surf" a single wave, or (2) the ion is not propelled with sufficient velocity to keep up with a single wave propagation and as a result the ion will "roll over" the initial wave and be captured by a subsequent wave. All ions which surf a single wave exit the TWIMS drift cell at the same velocity as that wave and are not mobility separated. As a result, only ions which are overtaken by the traveling waves are involved in mobility separation. The ion's velocity within the drift gas is described by its ion mobility, and so two hypothetical ions of different ion mobility will experience a different number of roll over events, with more roll-over events leading to longer retention of the slower ion. Consequently, an arrival time ion mobility spectrum in TWIMS is very similar to one generated from conventional DTIMS, with ion signal dispersed along the time axis from high to low mobility. The differences between DTIMS and TWIMS spectra were previously noted by Shvartsburg and Smith to be a result of the drift time in TWIMS scaling with the ion mobility in a quadratic relationship, whereas in DTIMS the drift time is linearly proportional to the ion mobility (Shvartsburg and Smith 2008).

In addition to the traveling wave velocity and the ion's intrinsic gas-phase mobility, the separation mechanism in TWIMS also depends on the gas pressure and wave amplitude, since raising the former or lowering the latter of these parameters will result in more roll-over events. It has been previously demonstrated that maximum ion mobility resolution in TWIMS occurs for the highest achievable drift gas pressure (3 Torr) and traveling wave voltage (40 V) in the instrumentation (Zhong et al. 2011), and so simulations presented in this work are limited in scope to these maximum resolution conditions.

EXPERIMENTAL

All ion simulations were conducted with the SIMION 8.1 ion optics simulator software package (Scientific Instrument Services, Ringoes, NJ) (Manura 2012). An accurate physical model of the electrode geometry of a second-generation TWIMS device (Waters Synapt G2, Manchester, UK) was constructed *in silico* (Figure 2A) based upon previously published dimensions (Zhong et al. 2011; Giles et al. 2011). The ion mobility separation region of the G2 TWIMS is replicated in the model and is comprised of 168 ring electrodes, each 0.5 mm thick with a 5 mm inner diameter. All electrodes are spaced 1.5 mm apart, yielding a total drift length of 254 mm from end to end. The TWIMS operates with two independent electrodynamic circuits. The first circuit applies a *ca.* 250 V (peak-to-peak), 2.8 MHz confining radiofrequency (RF) potential to the 168 TWIMS electrodes. This confining RF prevents ion losses due to normal off-axis radial diffusion and is not utilized for any ion mobility separation. The second circuit drives the traveling wave pulses which are applied to sets of 4 electrodes, then upon switching, is offset by 2 electrodes, such that the waves propagate with half pulse-width steps as they are dynamically pulsed across the drift cell (Figure 1B, left). A total of 42 traveling wave electrode sets are addressed in the TWIMS, with the same wave potential being applied to every fifth set of electrodes, resulting in a series of traveling waves across the drift region (Figure 2B).

In order to handle the two electrodynamic circuits in the simulation, a SIMION user program was written in house using the included Lua scripting language architecture. Briefly, this custom-written program allows for a user-defined wave amplitude and velocity to be applied for the traveling wave, while simultaneously superimposing the user-defined amplitude and frequency of the confining RF potential to every other electrode. The SIMION software as available from the vendor includes a hard-sphere collision model program (collision_hs1.lua) which computes the ion scatter trajectory and energy transfer based upon kinetic theory. This hard-sphere collision program is called within the custom-written electrodynamic user program, and allows for the gas temperature, pressure, mass and ion collision-cross section to be defined by the user. Other simulation parameters, such as the initial ion distribution (ion gate width), ion mass and charge are definable in the primary SIMION user interface. The Synapt G2 TWIMS instrument operates with a default 200 μsec ion gate, and thus the simulations presented in this work are conducted with a variable ion start time (denoted as "time-of-birth" in SIMION) between 0 and 200 μsec.

Three representative ion systems, benzoylmethylecgonine (cocaine), 3,4-methylenedioxy-*N*-methylamphetamine (MDMA), and alpha-methylphenethylamine (amphetamine), were selected for investigation in this work due to the availability of experimental reduced mobility values for the three drift gases evaluated (helium, nitrogen and argon) (Matz et al. 2002). The published reduced mobilities were converted to ion-neutral collision cross sections for use in the simulations using the Mason-Schamp relationship (Mason and Schamp 1958). Ion parameters are summarized in Table 1. Simulation results for the ion trajectories, arrival times, ion axial velocity and potential experienced by each ion were compiled for a minimum of 1000 ions per measurement in order to derive statistically relevant simulation data.

RESULTS AND DISCUSSION

Tables 2 and 3 summarize the TWIMS parameters used for all simulations presented in this report. As noted earlier, these parameters were chosen based on two criteria: typical values used in the TWIMS instrumentation and conditions which optimize experimental ion mobility resolution. For each of the three drift gases explored (helium, nitrogen and argon), a series of traveling wave velocities were investigated.

Characterizing the Ion Motion in TWIMS

In the following studies, ion motion was confined to the central axis of the TWIMS and the confining RF was not simulated in order to explore only the ion motion which results from the traveling wave. The traveling wave in TWIMS is characterized as a moving saddle point with a low potential region located at the central crest of the wave (Figure 2C). Thus, ions confined to the central axis are located at the traveling wave potential where ion rollover is most likely to occur.

Figure 3 contains the drift time results for the three ions in different drift gases as a function of the traveling wave velocity. For all ions in helium (solid line), the drift times are equal to that of a single traveling wave propagating through the drift region, indicative of ion surfing behavior. In these cases, the ion mobility is too fast for the traveling waves to overtake the ion, even at the highest velocities explored (2500 m/s). In contrast, ions in nitrogen and argon (dotted line traces in Figure 3) exhibit ion surfing behavior only at low traveling wave velocities (below ca. 500 m/s), where the mobility of the ion is sufficiently slow to follow the wave during each switching cycle. At higher wave velocities, the ion drift time deviates abruptly from the wave propagation time, which is indicative of ion roll-over taking place (Giles et al. 2010). In general, ions roll-over at lower wave velocities in argon than in nitrogen, which can be explained as a result of the lower ionic mobility in argon than

nitrogen. In turn, this is a result of the stronger drag force, momentum transfer, of the ion-argon collision. For both nitrogen and argon drift gas, ion drift time orders are indicative of their intrinsic ion mobilities, with amphetamine exiting the TWIMS drift region first, followed by MDMA and then cocaine.

The rate at which the ion drift time increases with the traveling wave velocity is non-linear at the transition region from surfing to roll-over (see inset, Figure 3), with the ion drift time initially increasing sharply as the TWIMS velocity increases. After *ca.* 700 m/s, there is a rough linear relationship between the ion drift time and the traveling wave velocity. This linear relationship can be explained as resulting from the increasing number of roll-over events at high traveling wave velocities contributing to a steady-state separation mechanism within the TWIMS drift region. An ion which undergoes many roll-overs during its transit through the TWIMS will sample various regions of the longitudinal potential energy surface of the traveling wave, whereas an ion at the verge of roll-over samples primarily the crest of the wave. This behavior can be better understood by sampling the velocity and voltage of a single ion as it transits the TWIMS simulation. Results from this analysis are given in Figures 4 and 5 for MDMA ions in nitrogen and argon drift gas, respectively. In Figures 4 and 5, three traveling wave velocities are sampled, representing the ion behavior for the three regimes of ion motion in TWIMS: (top) surfing only, (middle) the transition from surfing to intermittent roll-over, and (bottom) steady-state roll-over.

Surfing Region—For ions in nitrogen which surf a single wave at 400 m/s (Figure 4B, top), the ion velocity is characterized by a series of many repeat patterns (top panel, top trace) as the ion experiences the front potential of the same traveling wave as the traveling wave migrates across the drift cell. The ion potential in this case is represented by a repeating pattern of pulses (top panel, bottom trace) with a frequency equal to that of the switching time (*i.e.*, wave migration step) of the traveling wave. During surfing, the ion potential waveform exhibits a characteristic “tailing” as the ion rolls down the front of the wave to a low-potential well and is subsequently recaptured by the same wave as it pulses to the next set of electrodes. The ion potential never reaches zero, because even at the low-potential well between two traveling waves, the axial potential is still *ca.* 5 V in magnitude (Figure 2C, middle).

Transition Region—For ions which are characterized as transitioning between surfing and roll-over (MDMA 500 m/s, middle plot in Figure 4B) ion roll-over events occur only after several traveling wave switching cycles have been initiated. In this case, the ion velocity is steady during surfing, and abruptly drops to a negative velocity as the ion is overtaken by a traveling wave and subsequently rolls over the back of that wave in the negative longitudinal direction. The ion potential appears as a stepped pattern of pulses that increases in magnitude as each subsequent traveling wave captures the ion at a higher potential on the wave. Near the crest of the wave, the ion potential peaks at ca. 35 V, then abruptly drops to ca. 5 V as the wave switches from beneath the ion and the subsequent wave catches the ion beyond the crest, resulting in a roll-over event. This pattern repeats several times during the ion’s transit through the TWIMS drift region, resulting in an average lower velocity than an ion which surfs a single wave.

Steady Roll-over Region—Finally, for MDMA ions in nitrogen at 600 m/s (bottom plot, Figure 4B), ion motion is characterized as a series of repeating roll-over events, here repeating every 5^{th} switching cycle (4 pulses between roll-over events). For 500 m/s and beyond, the average ion potential reaches a steady state of *ca.* 20 V, resulting in the linear relationship between drift time and wave velocity exhibited in Figures 3 and 4. Figure 5 contains the simulation results for the MDMA ion behavior in argon drift gas. The same three regions of ion motion can be seen in both nitrogen (Figure 4) and argon (Figure 5),

with the only major difference being the wave velocity at which each region of motion occurs. Results for the other ions in nitrogen and argon exhibit the same three modes of ion motion, and are differentiated only by the TWIMS traveling wave velocity in which these transitions in ion motion occur.

Separation Efficiency in TWIMS

The separation efficiency in ion mobility is conventionally reported as the single peak resolving power value, where resolving power (R) is equal to the drift time (t) divided by the peak full width at half maximum (FWHM, Δt):

$$R = t/\Delta t \quad (1)$$

In some of the recent TWIMS literature, the resolving power is reported as a function of the collision cross-section ($\Omega/\Delta\Omega$), where Ω is related to t by an exponential relationship. Cross-section-based resolving power values for TWIMS are approximately twice that of drift time-based values (Zhong et al. 2011; Shvartsburg and Smith 2008). This is not the case for DTIMS where the cross-section-based resolving power scales linearly with the drift-time based values via the Mason-Schamp relationship. As previously noted by Shvartsburg and Smith, it should be cautioned here that the resolving power values obtained via equation 1 cannot be accurately compared between TWIMS and DTIMS due to the nonlinear nature of the ion velocity in TWIMS which results in the TWIMS-based resolving powers being species dependent (Shvartsburg and Smith 2008). Because no analytical expression exists to obtain cross-sections directly from TWIMS drift time measurements, we will use the time-based resolving power from equation 1 to quantify separation efficiency. Comparisons of multiple peaks will be used to gauge the obtainable resolution. In the following studies, the confining RF of the TWIMS model was utilized and ions were allowed to diffuse laterally within the drift region of the model.

The resolving power value can be obtained from the ion simulations by calculating the mean, standard deviation (σ) and FWHM of the drift time from an ensemble of ions ($N \geq 1000$, where $FWHM = 2\sigma(2\ln 2)^{1/2}$ assuming a Gaussian distribution). Figure 6 contains plots of the calculated resolving power values across the various TWIMS wave velocities. Error bars are obtained from triplicate ensemble runs. As observed previously, no separation occurs in helium, and so the resolving power values calculated from equation 1 for helium have no meaning with regards to separation efficiency. The resolving power values calculated for helium remain low due to the effect of the ion gate (200 μs), for the parameters explored in these simulations. Note here that the lack of observed separation in helium is primarily a result of the relatively high wave potential used in the simulations. Helium drift gas separations have been demonstrated previously for a first generation TWIMS instrument, which operates with lower wave potentials (Knapman et al. 2010). For nitrogen and argon, the three regions of ion motion can be observed in all resolving power plots, with a well-defined change in magnitude occurring between ion surfing and initial roll-over. Argon is predicted to exhibit higher resolving power values than nitrogen at the lower wave velocities immediately following this transition from ion surfing to ion roll-over (i.e., the second region of ion motion). As roll-over events become more frequent, the resolving power for both gases plateau, with argon exhibiting slightly lower resolving powers than nitrogen at the highest wave velocities investigated. From Figure 3, it is observed that the drift time increases linearly in this steady-state roll-over region (beyond *ca.* 1000 m/s). Thus, the resolving power behavior observed in Figure 6 is primarily due to the increasing FWHM value of the denominator in equation 1. The observation that resolving power decreases for argon at sufficiently high wave velocities is a result of the greater ion-gas collisional scatter in argon, contributing to a large FWHM. Finally, it is observed that the lower mobility ion species (cocaine) can achieve a slightly higher

resolving power value in TWIMS as compared with the higher mobility species (amphetamine) investigated. This is contrary to the expected scaling of higher resolving power for higher mobility species as predicted by Shvartsburg and Smith (Shvartsburg and Smith 2008). We propose that the reason for this discrepancy is a result of the rather large gate widths (200 μs) used for the simulations which serves to lower, to a greater extent, the achievable resolving power for the higher mobility species. Indeed, for the argon system, where drift times are significantly longer than in nitrogen, the differences in resolving power between the three ion systems explored are statistically insignificant. We have undertaken preliminary simulations which explore temporally narrower gate widths (100 and 10 μs, data not shown) and initial results have indicated that the contribution of the gate width to the resolving power for higher mobility species is significant due to the shorter drift times. We also note here that the general shape of the resolving power trends depicted in Figure 6 agree fairly well with the empirically-derived TWIMS data from Zhong et al., who observed a maximum time-based experimental resolving power of *ca.* 25 for a 490 Da pentapeptide (Zhong et al. 2011). The principle qualitative difference between the simulation results in this work and the experimental results of Zhong et al. is the experimentally-observed rapid decrease in resolving power for the higher wave velocities. Reasons for this discrepancy are the subject of a future manuscript. Simulation results obtained in this current work for all three ion systems explored exhibit maximum resolving power values between 16 to 18 which are achieved at intermediate wave velocities where ion roll-over reaches a steady state.

Figure 7 contains the simulated arrival time profiles for the ion systems investigated in this study. These profiles are obtained from a Gaussian fit of the histogrammed data of *ca.* 3000 individual ion drift times, which is subsequently binned into 1 μs time points. As noted earlier, no separation occurs in helium, and so the arrival time distributions for the different ion systems overlap (Figure 7A). In nitrogen, baseline separation is observed in the simulated spectra between the lowest mobility ion investigated (cocaine) and the two higher mobility ions (MDMA and amphetamine) for all wave velocities where separation occurs (above *ca.* 600 m/s). Slightly higher resolution is observed at higher wave velocity than lower, which underscores the importance of the steady state roll-over region of ion motion in TWIMS. Poor resolution is observed between the two high mobility ions (MDMA and amphetamine) which is a result of the very close difference in their intrinsic ion mobility values in nitrogen (ΔK_0 ~0.2 $cm^2V^{-1}s^{-1}$). While drift times increase with increasing wave velocities in TWIMS, as exhibited in Figure 3, any resolution gains from larger time dispersions is counteracted by the peak broadening due to normal ion-gas diffusion, leading to no significant improvement in resolution above a certain wave velocity. Interestingly, the profiles in the simulated spectra obtained for argon (Figure 7C) are nearly identical to the profiles obtained in nitrogen, suggesting that there is very little difference between conducting TWIMS in nitrogen or argon drift gas. The experimental results from Creaser and coworkers (Howdle et al. 2010) demonstrated that slightly higher resolutions can be achieved for argon than nitrogen for these relatively small ion systems. Their work utilized a first-generation TWIMS instrument which operates at lower pressures, wave heights, and wave velocities than the second generation TWIMS which is the focus of this present work. Indeed, at the lower wave velocities investigated in this work, slightly higher resolutions are observed in argon than in nitrogen (Figure 7B and 7C, 800 and 1000 m/s), however for sufficiently high velocities, there is no significant difference in resolution between nitrogen and argon. This conclusion is supported by the resolving power analysis depicted in Figure 6 where overall resolving power differences between nitrogen and argon are minor. Overall, Figure 7 predicts that despite no additional gains in resolving powers for higher wave velocities (Figure 6), the resolution of multiple ion signals is expected to improve.

Not shown in this report is the corresponding loss in sensitivity, which the simulations exhibit as an abrupt loss in ion transmission at very low and very high wave velocities due to insufficient ion capture within the TWIMS drift region. These mechanisms for ion loss can be mitigated somewhat with such strategies as increasing the ion injection potential or delaying the start of the traveling wave. Specific causes of ion losses in TWIMS are a part of ongoing studies in our laboratory.

CONCLUSIONS

A custom-written electrodynamic user program was developed for the SIMION ion trajectory simulation software and utilized to evaluate the TWIMS separation mechanism for three different drift gases (helium, nitrogen, and argon). Simulation results enable the visualization of three generalized regimes of ion motion in TWIMS: (1) ion surfing, (2) transition region, and (3) steady state ion roll-over. These regions of ion motion are accessed at different traveling wave velocities for nitrogen and argon drift gas, while in helium, only ion surfing occurs. For nitrogen and argon, an inversion in resolving power is observed as the wave velocity is scanned, specifically, argon exhibits higher resolving powers than nitrogen at lower wave velocities, while the opposite is observed at the higher velocities. The loss in resolving power for nitrogen and argon at the higher wave velocities is attributed to the contribution of ion-gas diffusion due to the longer retention of ions in the TWIMS drift region. Resolution analysis for simulated ion mobility spectra suggest that these slightly different resolving powers are only significant at the lower wave velocities, where differences in drift times can be exploited to effectuate a better separation. At higher wave velocities, the separations in both nitrogen and argon are predicted to be very similar.

Although these experiments are compared with those in the literature, empirical comparisons are underway for a broader set of conditions and will be the subject of a future report. It should also be cautioned that simulations were restricted to TWIMS parameters which were ultimately optimized for separations in nitrogen, and so there exists an inherent bias towards nitrogen drift gas when conducting the separation efficiency analyses. Previous TWIMS studies have suggested that utilizing lower pressures and wave potentials can improve selectivity for certain ion systems. Finally, there is strong motivation to extending these studies to other gas systems, and in particular, to gas mixtures, which is more relevant for the commercial implementation of TWIMS, where ion mobility is conducted in a mixture of nitrogen and helium. The extent to which Blanc’s law is applicable in TWIMS measurements is presently being evaluated.

Acknowledgments

JCM acknowledges David Manura (Scientific Instrument Services, Inc.) for insightful direction in developing the simulation model. JAM acknowledges initial discussions with Alex Shvartsburg (Pacific Northwest National Laboratory) on the separation mechanisms in traveling wave. Financial support for this work was provided by the National Institutes of Health (NIDA RC2DA028981), the Defense Threat Reduction Agency (HDTRAI-09-1-001), the National Science Foundation (MRI CHE-1229341), the Vanderbilt Institute of Chemical Biology, the Vanderbilt Institute for Integrative Biosystems Research and Education, and the Vanderbilt University College of Arts and Sciences.

REFERENCES

Dwivedi P, Wu C, Matz L, Clowers BH, Siems WF, Hill HH Jr. Gas-Phase Chiral Separations by Ion Mobility Spectrometry. Anal Chem. 2006; 78(24):8200–8206. [PubMed: 17165808]

Giles K, Pringle SD, Worthington KR, Little D, L. WJ, Bateman RH. Applications of a Traveling Wave-Based Radio-Frequency-Only Stacked Ring Ion Guide Rapid Commun Mass Spectrom. 2004; 18(20):2401–2414.

Giles K, Wildgoose JL, Langridge DJ, Campuzano I. A method for direct measurement of ion mobilities using a travelling wave ion guide. Int J Mass Spectrom. 2010; 298(1-3):10–16.

Giles K, Williams JP, Campuzano I. Enhancements in travelling wave ion mobility resolution. Rapid Commun Mass Spectrom. 2011; 25(11):1559–1566. [PubMed: 21594930]

Howdle MD, Eckers C, Laures AMF, Creaser CS. The effect of drift gas on the separation of active pharmaceutical ingredients and impurities by ion mobility-mass spectrometry. Int J Mass Spectrom. 2010; 298(1-3):72–77.

Knapman TW, Berryman JT, Campuzano I, Harris SA, Ashcroft AE. Considerations in experimental and theoretical collision cross-section measurements of small molecules using travelling wave ion mobility spectrometry-mass spectrometry. Int J Mass Spectrom. 2010; 298(1-3):17–23.

Manura, DJ. SIMION 8.1.1.14 incorporating the “Collision Model HS1” user program. LUA edn.. Scientific Instrument Services, Inc.; Ringoes, NJ: 2012.

Mason EA, Schamp HW. Mobility of gaseous lons in weak electric fields. Ann Phys. 1958; 4(3):233–270.

Matz L, Hill H, Beegle L, Kanik I. Investigation of drift gas selectivity in high resolution ion mobility spectrometry with mass spectrometry detection. J Am Soc Mass Spectrom. 2002; 13(4):300–307. [PubMed: 11951967]

Pringle SD, Giles K, Wildgoose JL, Williams JP, Slade SE, Thalassinos K, Bateman RH, Bowers MT, Scrivens JH. An investigation of the mobility separation of some peptide and protein ions using a new hybrid quadrupole/travelling wave IMS/oa-ToF instrument. Int J Mass Spectrom. 2007; 261(1):1–12.

Reid Asbury G, Hill HH Jr. Using Different Drift Gases to Change Separation Factors in Ion Mobility Spectrometry. Anal Chem. 2000; 72(3):580–584. [PubMed: 10695145]

Ruotolo BT, McLean JA, Gillig KJ, Russell DH. Peak capacity of ion mobility mass spectrometry: the utility of varying drift gas polarizability for the separation of tryptic peptides. J Mass Spectrom. 2004; 39(4):361–367. [PubMed: 15103649]

Rusyniak M, Ibrahim Y, Alsharaeh E, Meot-Ner M, El-Shall MS. Mass-Selected Ion Mobility Studies of the Isomerization of the Benzene Radical Cation and Binding Energy of the Benzene Dimer Cation. Separation of Isomeric Ions by Dimer Formation. J Phys Chem A. 2003; 107(38):7656–7666.

Shvartsburg AA, Smith RD. Fundamentals of Traveling Wave Ion Mobility Spectrometry. Anal Chem. 2008; 80(24):9689–9699. [PubMed: 18986171]

Zhong Y, Hyung S-J, Ruotolo BT. Characterizing the resolution and accuracy of a second-generation traveling-wave ion mobility separator for biomolecular ions. Analyst. 2011; 136(17):3534–3541. [PubMed: 21445388]

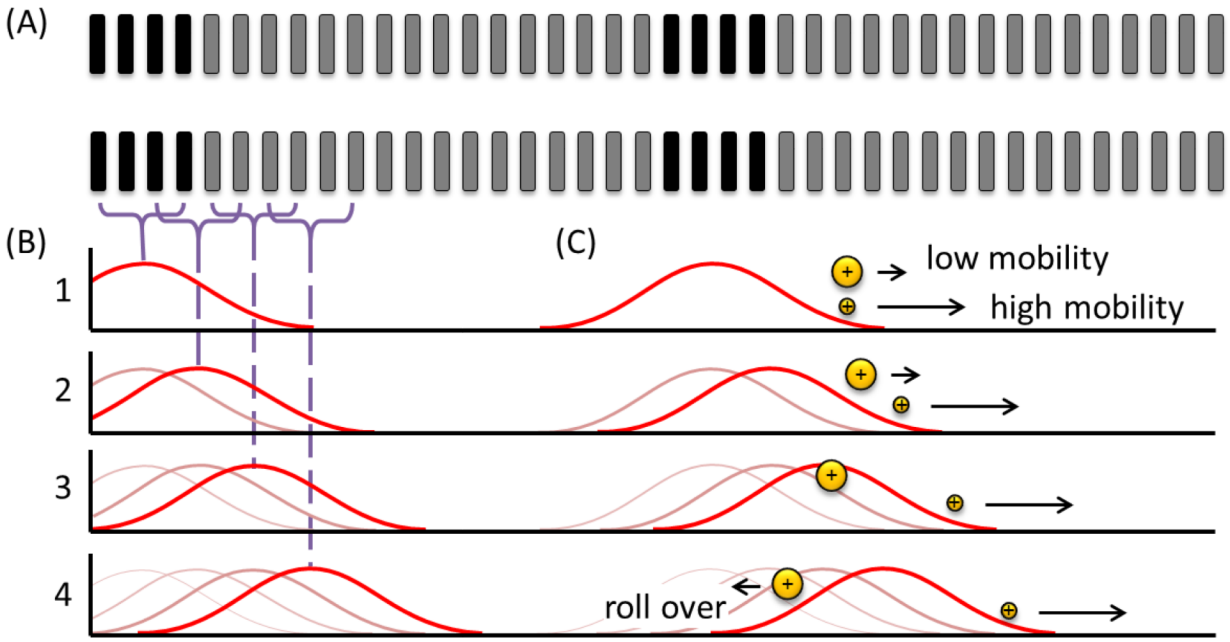

Fig. 1.

Overview of the separation mechanism of TWIMS. (A) The TWIMS drift cell is comprised of a stack of rings in a similar configuration as a DTIMS drift cell. The first 40 of 168 electrodes which comprise the second-generation commercial TWIMS drift cell is depicted here. (B) A traveling wave potential is applied to sets of four electrodes at one time, and systematically offset by two electrodes, creating a smooth transition between each wave cycle (1-4). (C) Ion separation in TWIMS relies on lower mobility ions rolling over the traveling waves more frequently than higher mobility ions, causing the former to be retained longer within the drift region.

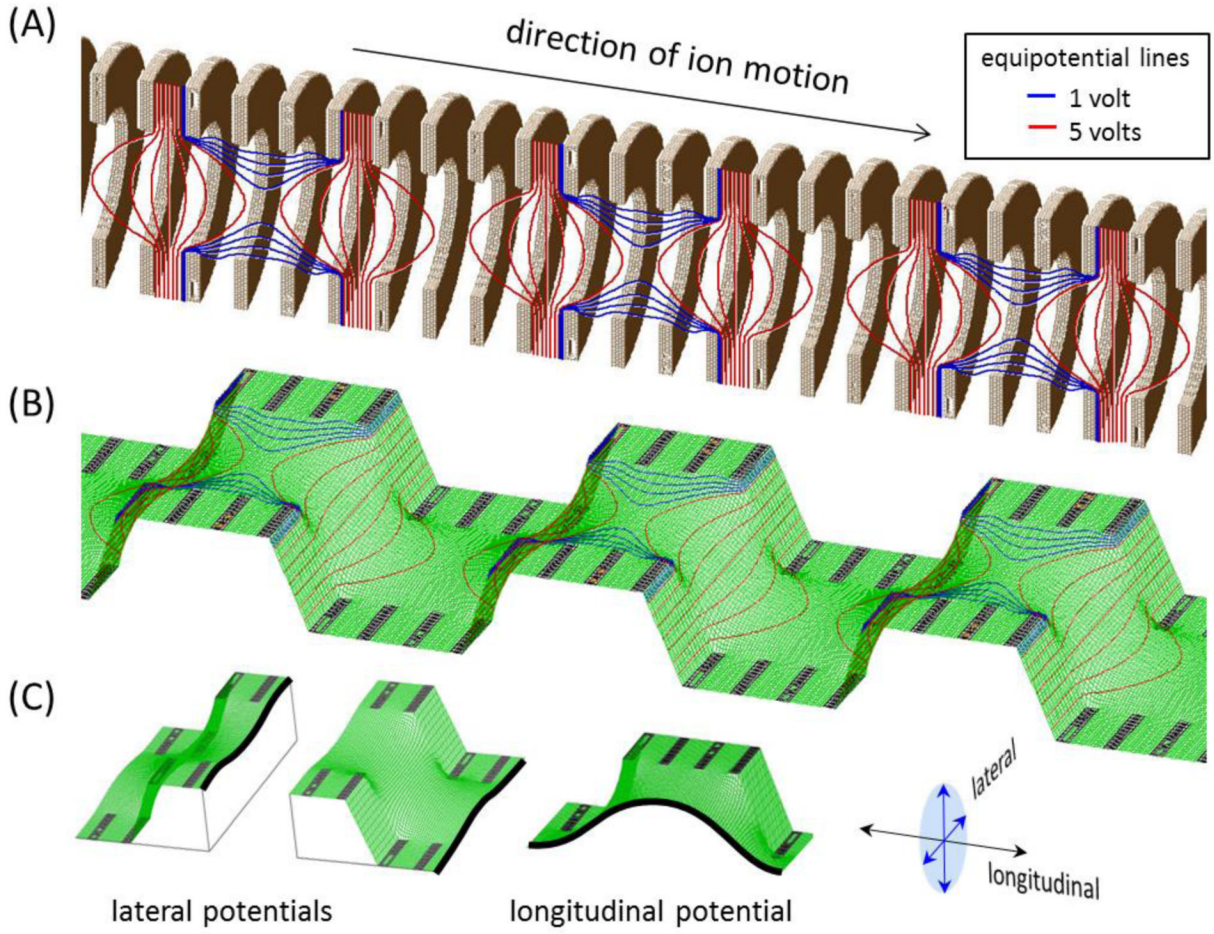

Fig. 2.

Details of the ion simulation model. (A) A cutaway of 24 central electrodes out of 168 total. Equipotential lines corresponding to one step cycle of a 40 V applied traveling wave is indicated along the axis of the model. (B) Potential energy mesh surface illustrating the repeating pattern of traveling waves applied in the second-generation TWIMS. (C) Cutaways of the potential energy surface along the (left) lateral and (right) longitudinal directions.

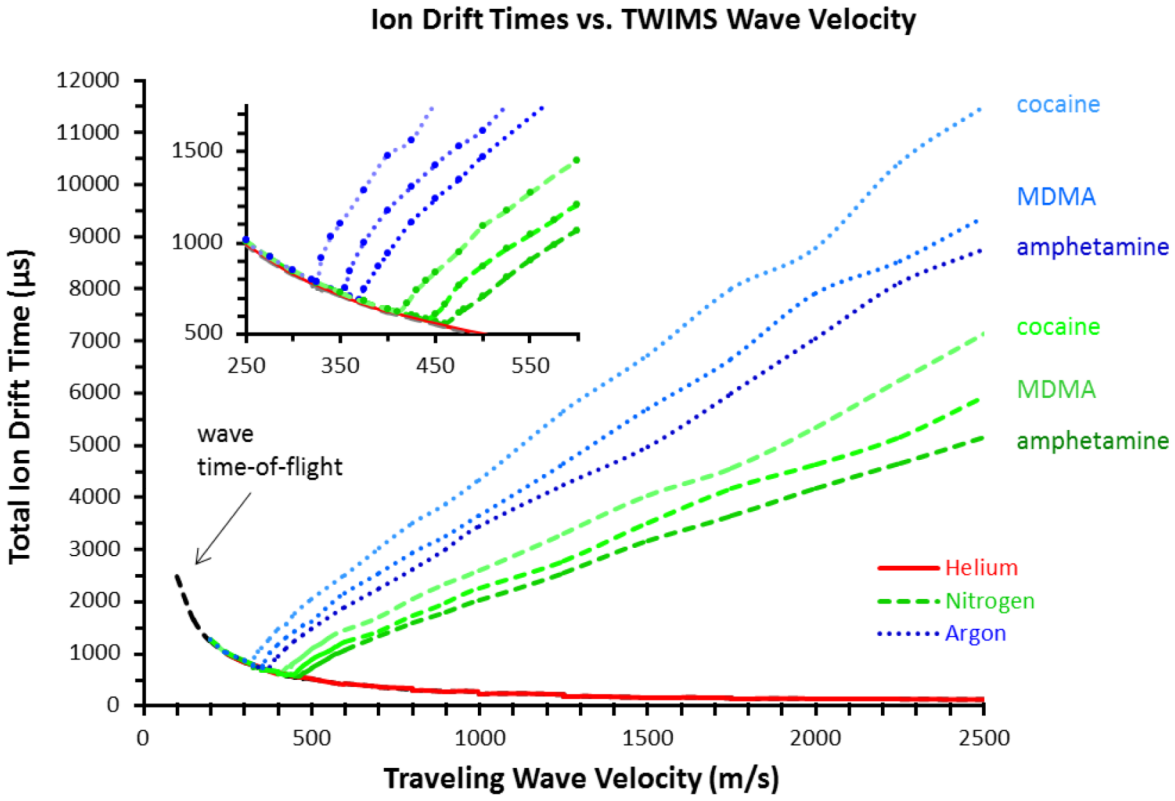

Fig. 3.

A plot of total ion drift time vs. the traveling wave velocity for the three ions in the three different drift gases. At low wave velocities, all ions surf on a single traveling wave. Increasing wave velocities initiate ion roll-over behavior for nitrogen and argon, whereby the ion time-of-flight deviates from the wave time-of-flight. No ion roll-over is observed in helium for the conditions explored in the simulations (40 V wave height, 3 Torr drift gas pressure). A blowup of the transition region (inlay plot) shows that the transition from ion surfing to ion roll-over is abrupt.

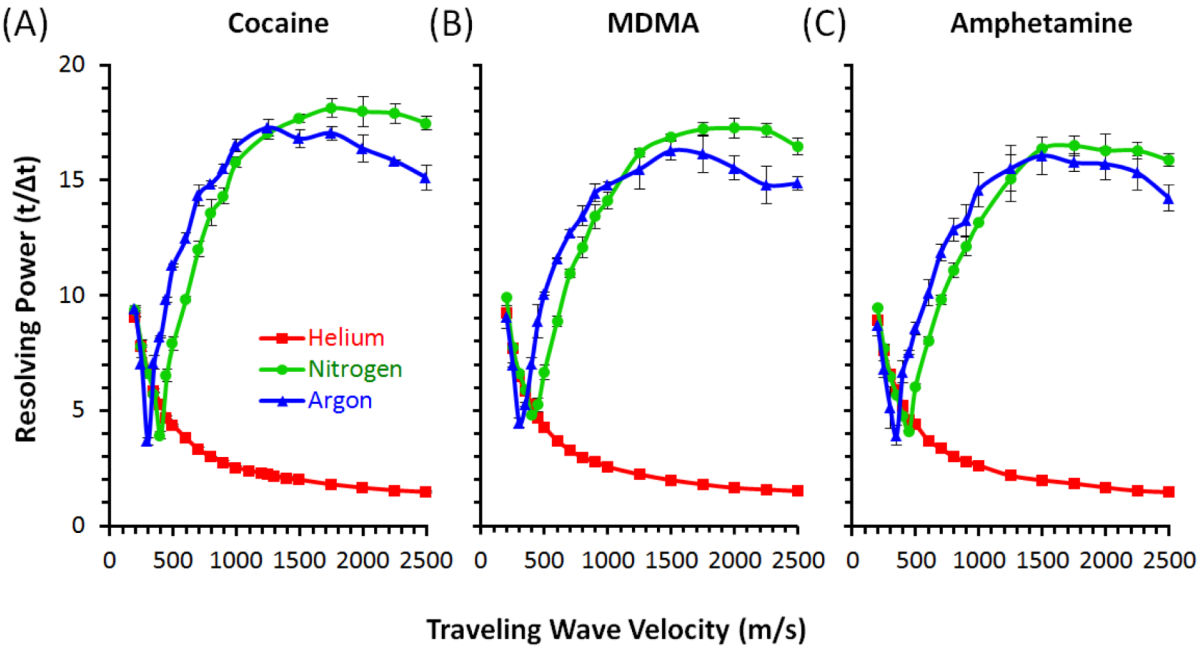

Fig. 4.

Analysis of TWIMS ion motion using the electrodynamic simulation model. (A) Arrival time plot as a function of the wave velocity for MDMA ions in nitrogen drift gas. The three regimes of ion motion in TWIMS is indicated along with a fit to the linear region above 500 m/s. (B) Combination plots of the ion velocity and ion potential during a single ion simulation run. Three TWIMS velocities are sampled between 400 and 600 m/s, representing the transition from ion surfing behavior (400 m/s, top plot), to ion roll-over behavior (bottom plots). The ion velocities (corresponding to the left y-axis) are the top trace of each plot, while the ion potentials (right y-axis) correspond to the lower trace in each plot. Horizontal dotted lines represent the mean ion velocity and ion potential across the entire simulation.

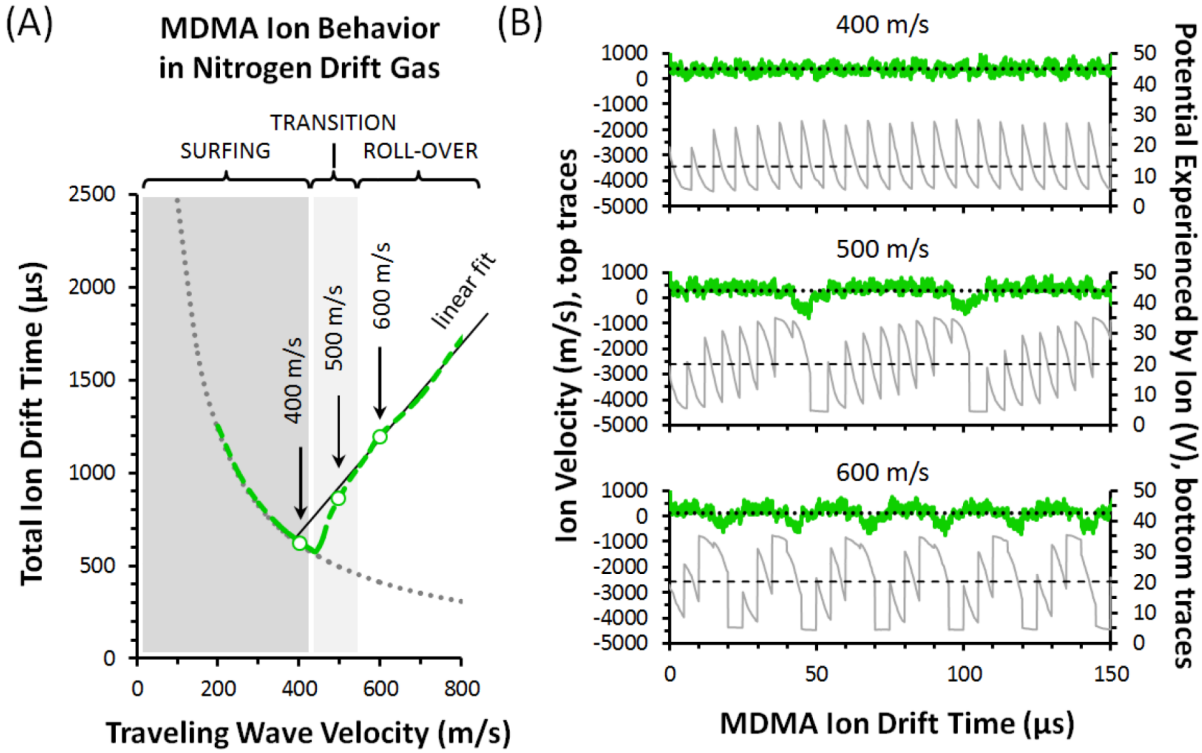

Fig. 5.

Ion motion analysis for MDMA in argon drift gas. (A) A plot of arrival time as a function of the traveling wave velocity indicates the same three regions of ion motion as observed in nitrogen (indicated at the top of the plot). (B) Ion velocity and ion potentials sampled from each of the three regions of ion motion exhibit the same patterns as observed in nitrogen. In the transition and roll-over regions, the ion potential averages 20 V and the mean ion velocity is much slower than the wave velocity.

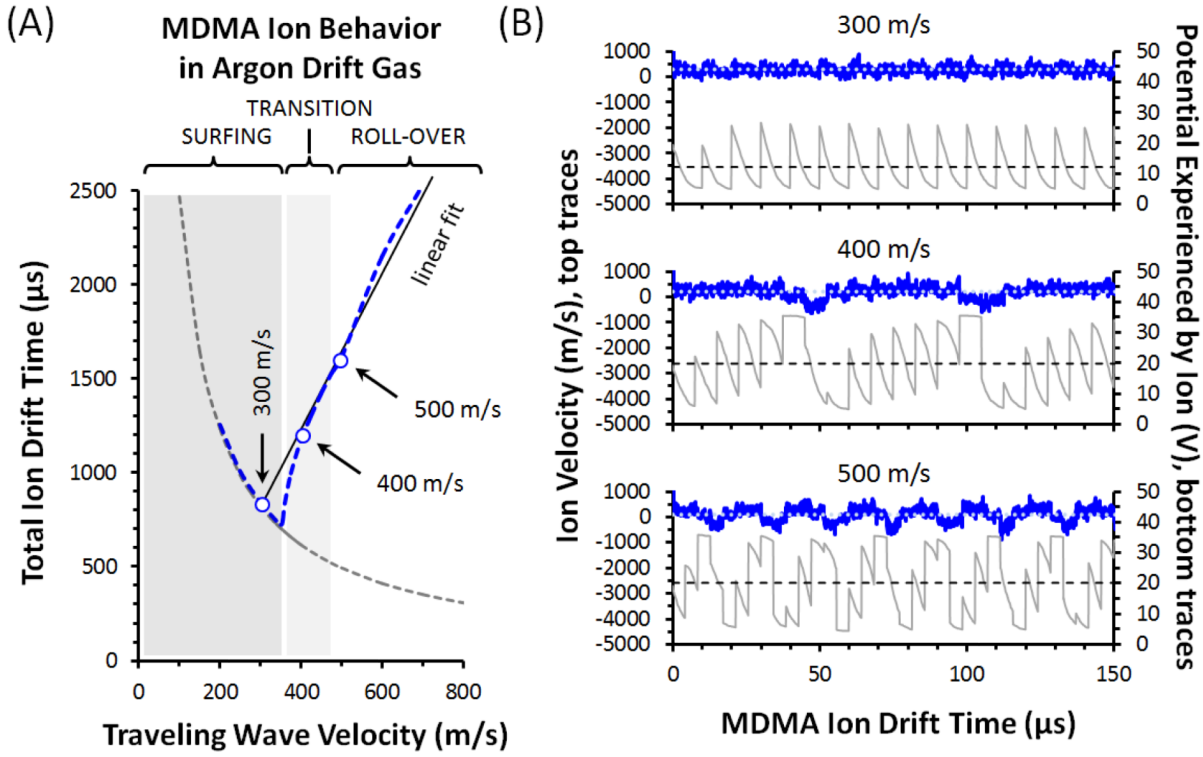

Fig. 6.

Resolving power curves as a function of the TWIMS traveling wave velocity. Plots are generated from the simulated drift times of (A) cocaine, (B) MDMA, and (C) amphetamine in helium, nitrogen and argon drift gas. Error bars represent the deviation from three datasets comprised of *ca.* 1000 ion runs each. No separation is observed in helium, while both nitrogen and argon exhibit similar resolving power trends. An inversion in resolving power occurs whereby argon exhibits slightly higher resolving powers at the lower wave velocities, and nitrogen leading to higher resolving powers at the higher velocities.

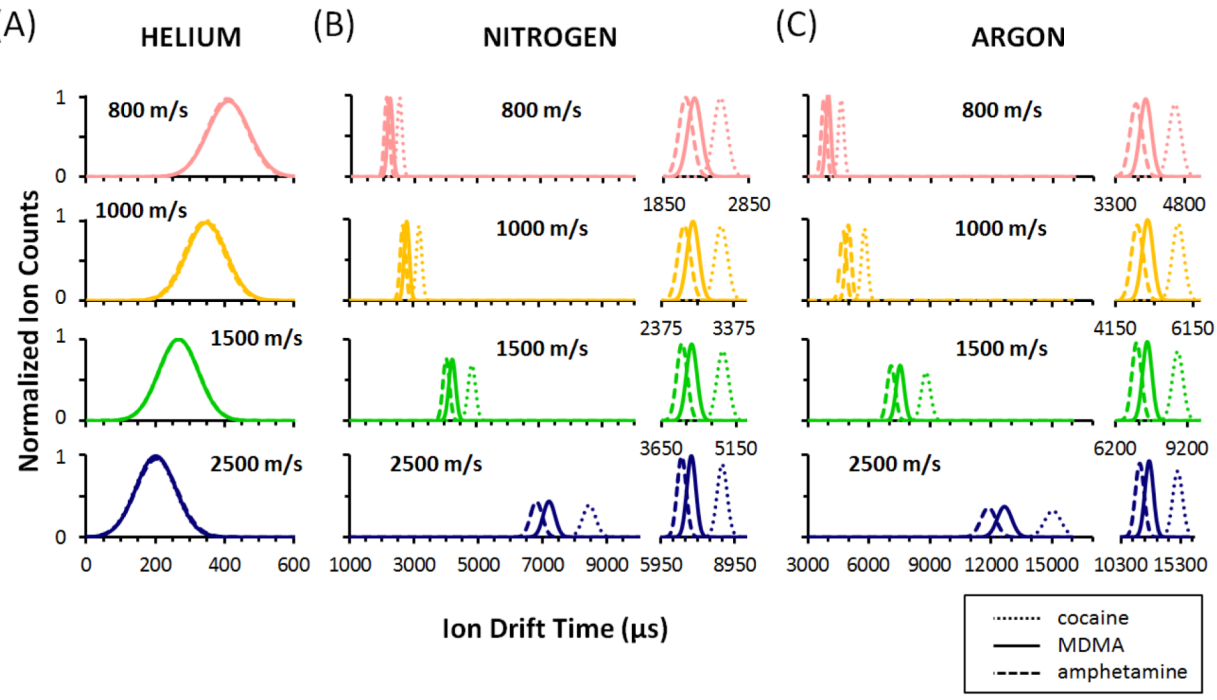

Fig. 7.

Simulated ion mobility spectra obtained for a mixture of the three ions investigated in (A) helium, (B) nitrogen, and (C) argon drift gas. Plot rows represent selected traveling wave velocities from 800 m/s (top) to 2500 m/s (bottom). Profiles represent a Gaussian fit of the histogrammed drift times and are normalized to the same ion counts. Expanded profiles for nitrogen and argon (right panels) are scaled to both the same magnitude and relative arrival times between the first (amphetamine) and last (cocaine) distributions. As with the resolving power trends, the resolution observed for argon is slightly higher than for nitrogen at the lower wave velocities and both gases exhibit virtually identical separations at the higher wave velocities.

Table 1

Details of the ion systems modeled in this work.

	mass [Da]	Reduced mobility, K0 [cm2·V-1·sec-1]			Collision Cross-Section [Å2]		
		Helium	Nitrogen	Argon	Helium	Nitrogen	Argon
benzoylmethylecgonine (cocaine)	303.35	3.382	1.063	0.933	47.3	150.4	171.3
3,4-methylenedioxy-N-methylamphetamine (MDMA)	193.25	4.464	1.363	1.211	36.7	120.1	135.1
alpha-methylphenethylamine (amphetamine)	135.21	5.37	1.557	1.393	31.3	107.9	120.6

Experimentally measured reduced mobility values were obtained from Reference 9.

Table 2

TWIMS parameters used in this study.

TWIMS Drift Length	(cm)	25.4
Traveling Wave Potential	(V)	40
Ion Storage Time (ion gate)	(μs)	200
Confining RF Frequency	(MHz)	2.8
Confining RF Potential (peak-to-peak)	(V)	250

Table 3

Traveling wave velocities and their corresponding temporal values investigated in this work.

Traveling Wave Velocity	(m/s)	200	300	400	500	600	700	800	900	1000	1250	1500	1750	2000	2250	2500
Dwell Time for a Single Wave	(μs)	15	10	7.5	6	5	4.3	3.8	3.3	3	2.4	2	1.7	1.5	1.3	1.2
Time-of-flight for a Single Wave	(μs)	1270	847	635	508	423	363	318	282	254	203	169	145	127	113	102